

Accepted Manuscript

Gas phase dispersion/mixing investigation in a representative geometry of gas-liquid upflow moving bed hydrotreater reactor (mbr) using developed gas tracer technique and method based on convolution/ regression

Vineet Alexander, Hamza Albazzaz, Muthanna Al-Dahhan

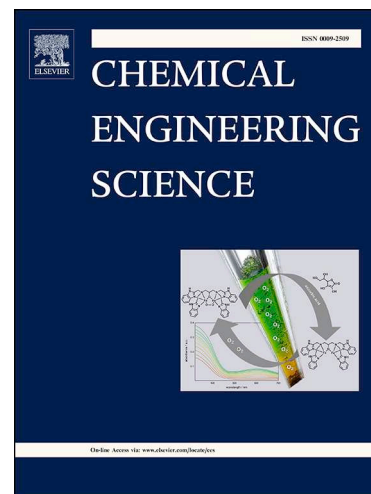
PII: S0009-2509(18)30726-7
DOI: <https://doi.org/10.1016/j.ces.2018.10.013>
Reference: CES 14545

To appear in: *Chemical Engineering Science*

Received Date: 5 July 2018
Accepted Date: 10 October 2018

Please cite this article as: V. Alexander, H. Albazzaz, M. Al-Dahhan, Gas phase dispersion/mixing investigation in a representative geometry of gas-liquid upflow moving bed hydrotreater reactor (mbr) using developed gas tracer technique and method based on convolution/ regression, *Chemical Engineering Science* (2018), doi: <https://doi.org/10.1016/j.ces.2018.10.013>

This is a PDF file of an unedited manuscript that has been accepted for publication. As a service to our customers we are providing this early version of the manuscript. The manuscript will undergo copyediting, typesetting, and review of the resulting proof before it is published in its final form. Please note that during the production process errors may be discovered which could affect the content, and all legal disclaimers that apply to the journal pertain.



GAS PHASE DISPERSION/MIXING
INVESTIGATION IN A REPRESENTATIVE
GEOMETRY OF GAS-LIQUID UPFLOW MOVING
BED HYDROTREATER REACTOR (MBR) USING
DEVELOPED GAS TRACER TECHNIQUE AND
METHOD BASED ON CONVOLUTION/
REGRESSION

Vineet Alexander¹, Hamza Albazzaz², Muthanna Al-Dahhan^{*,3}

^{1,*}*Department of Chemical & Biochemical Engineering, Missouri University of Science
and Technology, Rolla, MO-65409*

²*Kuwait Institute for Scientific Research, Safat, Kuwait*

³*Cihan University, Erbil, Iraq*

Email: ¹vineet.alexander@gmmail.com, ^{,3}aldahhanm@mst.edu*

Abstract

Gas dispersion studies has been executed for the catalyst bed section of a representative geometry of scaled-down industrial Moving Bed Hydrotreater Reactor (MBR). The catalyst bed of MBR is modeled using Axial Dispersion Model (ADM) and its parameters gas dispersion coefficient (D_g) and pecelet number (Pe) are estimated using Residence Time Distribution (RTD) and implementing a methodology based on convolution and regression. Additionally, dimensionless variance (σ_D^2) for the catalyst bed is also measured using RTDs first and second moments to compare with those findings of ADM model. This study is conducted at the varying flow rates of gas and liquid including scaled down operating conditions. The results of D_g , Pe , and σ_D^2 indicate that bed behaves as a packed bed for low liquid flow rate and moves towards three-phase fluidized bed for increasing liquid flow rate. Overall the gas phase behavior is seen to be in plug flow for all the operating conditions, with relatively high dispersion/mixing in packed bed state. Scaled down flow conditions is seen to be best in terms of gas dispersion/mixing and catalyst utilization.

Keywords: Residence Time Distribution (RTD), Moving Bed Reactor (MBR), Gas Tracer, Gas Dispersion Coefficient, Peclet Number, Axial Dispersion Model (ADM)

1. Introduction

Uplow moving bed reactor is a hydrotreater and used for removal heavy metal content from crude oil. It is usually a replacement for fixed bed Hydrodemetalization reactor, which is guard reactor to the fixed bed residual desulfurization (RDS) unit [1]. This reactor has a catalyst bed section having a conical bottom and plena below the cone. The operating parameters are upflow movement of resid oil and hydrogen over hydrodemetalization catalyst (HDM), with flow conditions to limit the bed expansion to 10 percent of catalyst bulk volume [2]. The specialty of MBR is the conical bottom, which enables removal of spent catalyst under operation, this increases the run time of the reactor without shutdown. At industrial conditions, the catalyst removal takes place few times per week and that too in small increment, rest all time the reactor behaves as upflow packed bed or expanded bed. It is usually operated at a low linear velocity of the mixed feed to avoid substantial expansion (or contraction) of the bed [2]. The expanded bed or ebullated bed can improve the distribution of phases cross-sectionally but is usually not preferred due to increased catalyst attrition, bed mixing, increased reactor length for the desired conversion [2] at these conditions.

The major problems seen for this kind of reactor at industrial scale are catalyst coking, agglomeration, and early shutdown. The primary factors for these unwanted phenomena is maldistribution of phases [2] which can result in unwanted mixing behavior of phases or the coke reaction related to catalyst type and its reaction, which is the least studied reaction, but this study focus is mixing. The mixing of a phase within the reactor is conventionally classified as micromixing and macromixing [3]. Micromixing is the mixing occurring at the molecular level, and it depends on the intimacy of two nearby molecules. Micromixing parameter such as molecular diffusion is hard to estimate using experimental measurement technique. The macromixing phenomena is at a scale where the individual phase can be considered as an entity moving with convective dispersion and bulk flow and dispersing along axial, radial and angular direction. It is not feasible to measure the local velocity field profile at every possible local position within the reactor

33 to quantify macromixing. Therefore, RTD concept is used, where a tracer is
34 injected and detected **at** the boundaries of test section and obtained RTD
35 curve quantifies the dispersion/mixing in terms of its spread [4]. RTD's are
36 comprehended using mass balance model having dispersion coefficient param-
37 eter, which lumps the non-ideality in terms of the convective dispersion
38 and molecular diffusion, which dictates the spread in the RTD curve. Dis-
39 persion coefficient is an important design parameter, as the performance of
40 any reactor depends on inter and intraparticle rate process for heat and mass
41 transfer which is directly related to the mixing of phases. Hence, it is es-
42 sential to determine the dispersion parameters and to integrate it with the
43 intrinsic kinetics and other mass, and heat transfer parameters to yield re-
44 actor design and models, that account for certain extent of non ideality [3].
45 The knowledge of gas phase dispersion/mixing quantified in terms of disper-
46 sion coefficient is useful, as in most of the mathematical model for upflow
47 packed or fluidized bed the axial dispersion and film diffusion describe the
48 bulk phase mass transfer [5].

49 There are no studies in the open literature on gas dispersion/mixing study
50 in MBR reactor having a conical bottom. The closest possible literature is for
51 gas mixing studies in upflow packed bed [[6], [7], [8]], and expanded/fluidized
52 bed [9], due to bed behavior of MBR from packed bed to three phase fluidized
53 bed based on the flow conditions of the phases. All these studies used RTD
54 concept and obtained dispersion coefficient using either moment method or
55 modeling the test section with appropriate mass balance model having dis-
56 persion parameter. In moment method, the second moment (variance) of
57 the RTD [10] is matched with the equation of variance for different bound-
58 ary conditions [11]. In reactor modeling approach, the obtained RTD is fitted
59 for mixing parameters of a model describing the mass flow behavior inside
60 the test section. At macromixing level, the extreme flow conditions can be
61 modeled using plug flow for no mixing/dispersion, and CSTR for completely
62 mixed flow [3]. If the flow is not much deviating from the plug flow, then Ax-
63 ial Dispersion Model (ADM) and its many derivatives are the most common
64 model used to describe the flow behavior [[3], [4]].

65 In many cases, such as in hydrotreaters, the area of interest (catalyst bed)
66 is accompanied by additional volumes (plena). Here, by injecting tracer at
67 the inlet and detecting at the outlet of the entire reactor will not give the re-
68 quired RTD information of the test section (catalyst bed). In these instances
69 one injection and two-point measurement methods are implemented.

70 In one injection and two-point measurement method, is an injection-

71 sampling concept in which an injected tracer at the inlet of the reactor is
72 sampled before and after the test section, and the difference in the variance
73 of the two obtained RTD gives the effective dispersion coefficient of the test
74 section. It is based on the assumption that the spreading of tracer or variance
75 of the curve is linearly changing along the reactor [[11], [12]]. [6] used this
76 approach with a step input to find the mixing of gas phase in a two-phase
77 packed bed column.

78 Luhan([13]) advanced one injection and two-point detection method by
79 integrating this injection-sampling concept with convolution and regression
80 principle. In this approach the test section is modeled with appropriate
81 model and the solution of the model is considered as the RTD response
82 of the test section, the response of the test section is convoluted with the
83 RTD signal sampled at the inlet. The convoluted signal is theoretical RTD
84 at the outlet of the test section based on the model parameters and for
85 the inlet boundary condition obtained by sampling at inlet of test section.
86 The theoretical output response is regressed with actual output response
87 obtained from sampling of tracer at the outlet of test section for minimum
88 error to estimate mixing parameters. [13] implemented this method on a
89 slurry bubble column reactor and [14] followed this approach on pebble bed
90 reactor to obtain dispersion parameters of gas phase in plenum and bed zone
91 (test section) of these reactors. They also measured the RTD curve along
92 the radial profile at the inlet of the bed section and found similar curves
93 radially. The significance of this radial study is that it shows the tracer
94 from the plenum is evenly distributing to the bed section. The one injection
95 and two-point measurement method is not applicable to the cases where the
96 plenum are not evenly distributing the phases to the bed section. As a single
97 point measurement at the outlet of the plenum does not represent the actual
98 flow behavior of the plenum. The similar scenario is observed in MBR due
99 to conical bottom of the catalyst bed (test section) and complex internal of
100 plenum.

101 The solution to this problem is an alternative injection-sampling concept
102 called two-point/multiple injections and one detection method. In which
103 the tracer is injected at inlet and outlet of the test section and detected
104 at the outlet of the reactor after a mixing cup to ensure even distribution
105 of tracer at the detection cross-sectional plane [15]. [16] used this method
106 and compared with one injection and two-point detection method, and found
107 both method yield similar results when experimental RTDs are interpreted
108 with theoretical models using danckwerts boundary.

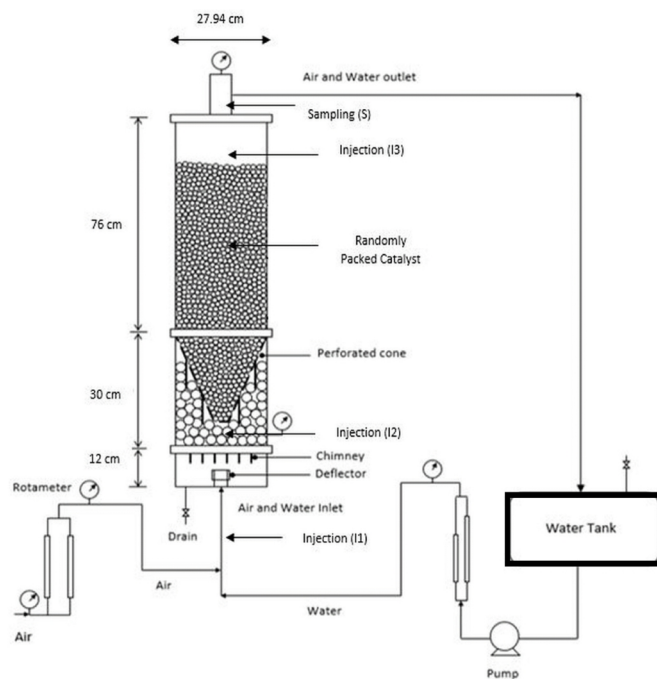


Figure 1: Schematic diagram of scaled down MBR setup for gas dynamics studies

109 This study focuses on investigating the gas mixing behavior at various
 110 flow condition in the catalyst bed section of MBR reactor. The approach
 111 followed is a injection-sampling concept based on multiple injection and one
 112 detection method along with convolution-regression principle approach pro-
 113 posed by [13]. This objective is achieved by developing a gas tracer experi-
 114 mental facility for MBR based on the experimental facility developed by [13]
 115 for slurry bubble column reactor and [14] for pebble bed reactor. This exper-
 116 imental facility has multiple injections and one sampling port and provisions
 117 to obtain the RTD curve only for gas phase from the two-phase upflow at
 118 different sections of the MBR. The RTDs of different sections along with
 119 ADM and Ideal CSTR-PFR model for packed bed and plena respectively, is
 120 used with convolution-regression to estimate dispersion/mixing parameters
 121 of catalyst bed section.

122 **2. Experimental Setup**

123 The experimental set-up of the moving bed hydrotreater (MBR) reactor
 124 is scaled down to pilot-plant scale from industrial scale based on hydrody-
 125 namic and geometric similarity. The scaled down flow operating condition
 126 is obtained by matching the LHSV and gas-liquid volumetric flow rate ratio
 127 with the industrial operating conditions.

Table 1: Reactor design parameters and experimental condition for gas dispersion/mixing study

| Parameters | Value/Range | Comment |
|-------------------------------------|----------------------------|---|
| Column Diameter | 27.94 <i>cm</i> | Height from top of the cone to the top of the bed at no flow rate |
| Column Height | 118 <i>cm</i> | |
| Bed Height | 63 <i>cm</i> | |
| Catalyst | 3 <i>mm</i> Diameter | Bulk Density (570 <i>Kg/m³</i>) |
| Liquid (Water) Superficial Velocity | 0.01 to 0.4 <i>cm/sec</i> | By matching LHSV of industrial and scaled down reactor |
| Gas (Air) Superficial Velocity | 1.28 to 5.13 <i>cm/sec</i> | |
| Scaled Down Liquid Flow Rate | 0.0175 <i>cm/sec</i> | |
| Scaled Down Gas Flow Rate | 7.7 <i>cm/sec</i> | By matching Gas/liquid volumetric flow rate of industrial and scaled down reactor |

128 The schematic of the pilot plant scale reactor is shown in Figure 1. The

129 reactor is a plexiglass column of height 118 cm and the internal diameter of
130 29.7 cm. It is divided into three sections by distributor plate and conical
131 bottom. The parts below conical bottom are called plena, and it is further
132 divided into lower and upper plenum. The lower plenum consists of the de-
133 flector and 19 chimneys. The chimneys are attached to the distributor in
134 triangular pitch and have an additional side hole opening just below the dis-
135 tributor plate (Figure 1). The upper plenum is the compartment between the
136 conical bed and the upper plenum wall which is tightly packed with passive
137 spheres to cover the entire region between the conical bottom and distribu-
138 tor plate. Above the conical bottom is bed section, which is the region from
139 conical base to the top of the bed at cylindrical column, It is filled with 3mm
140 industrial grade HDM (Hydrodemetallization) catalyst. The conical bottom
141 is perforated, and perforations are small enough to avoid catalyst plugging.
142 At industrial operation, the catalyst withdrawal is facilitated through the
143 cone.

144 The ancillaries for the reactor are gas and liquid rotameters, liquid pump,
145 and water tank. This reactor operates in upflow state, with premixed gas-
146 liquid which is under control by rotameters are fed mixed into the deflector
147 of the lower plenum. For scaled down operating conditions the flow profile
148 inside the lower plenum will have a gas pocket around the chimneys side hole.
149 The gas penetrates through the side hole, and liquid enters through main hole
150 of chimney at its bottom both are mixed below the distributor and ejects as
151 a spray to upper plenum. The passive spheres in the upper plenum distribute
152 the incoming phases and are fed to the bed section through the perforated
153 cone. The distributed stream maintains the bed in packed or expanded bed
154 state based on the flow conditions. For scaled-down operating condition, the
155 bed behaves as packed bed with slight expansion at the top of the bed.

156 In this study, the gas dispersion is investigated by varying flow rate of gas
157 and liquid and at the scaled-down experimental condition. The dimensions
158 of the experimental setup and operating conditions used in this study are
159 shown in the Table 1.

160 **3. Gas Dynamic Tracer Technique for Evaluation of the Residence** 161 **Time Distribution (RTD) of the gas phase in the gas-liquid up-** 162 **flow MBR**

163 The residence time distribution (RTD) concept is developed long time
164 ago for flow evaluation of reactor by developing a model for the reactor and

165 quantification by RTD [[17], [11], [18]]. Its simplicity has made it an useful
166 part of engineering applications, but simplicity lies within a particular range
167 of applications such as single phase small-scale reactors. The complication
168 arises when the multiphase flow is encountered; it can be difficult to separate
169 a phase from a mixture and analyze them for tracer for RTD determination
170 [18]. The trouble increases when reactors have plena, and the RTD is only
171 needed for the reactor-bed section, where the conversion occurs. To over-
172 come these difficulties, [13] developed dynamic gas tracer experimental and
173 mathematical approach for slurry bubble column. The developed dynamic
174 gas tracer experimental technique and a mathematical approach for a slurry
175 bubble column reactor is used and implemented by [14] on a pebble bed
176 reactor. Here we extend this to upflow moving bed reactor (MBR). The de-
177 veloped tracer technique for MBR can separate gas phase from the mixture
178 of gas-liquid.

179 *3.1. Dynamic Gas Tracer Technique*

180 Figure 2 shows the components of the gas tracer technique. Gas tracer is
181 analyzed using a Thermal Conductivity Detector (TCD- Gow MAC 20 series)
182 (Figure 2a). Helium is used as a gas tracer, which is non-reactive, non-
183 transferable to liquid phase [13], and having the physical property similar
184 to the gas phase (air) [3]. Different kind of gas tracer are used for RTD
185 studies based on the detection equipment and is summarized by [3]. Nitrogen
186 (Figure 2b) is reference gas for the TCD. Water pump (Figure 2c) removes
187 tracer laden gas-liquid mixture out of the reactor. In house developed Gas-
188 liquid separator (Figure 2d (1)) separates gas from the liquid using a gas-
189 pump (Figure 2d) and before gas pump there is a moisture remover (Figure
190 2c). These components along with data acquisition system (Gow-Mac) and
191 reactor forms gas dynamic tracer system.

192 *3.2. Gas Tracer System of MBR*

193 Figure 3 shows the gas tracer system of MBR. Helium is injected through
194 injection tubes (I1, I2, I3), detailed explanation of the injection and sampling
195 is given in section 4.1. Compressed helium gas cylinder (Figure 2b) is con-
196 nected to a solenoid valve using nylon tube (0.5 inches), and the connection
197 continues to injection points. The solenoid valve is controlled by a digital
198 timer and set for 0.5 sec opening interval; this provides a pulse injection.
199 The tracer sticks to the gas phase and follows its path along with the liquid
200 phase. The gas-liquid mixture enters into mixing cup as shown in the Figure

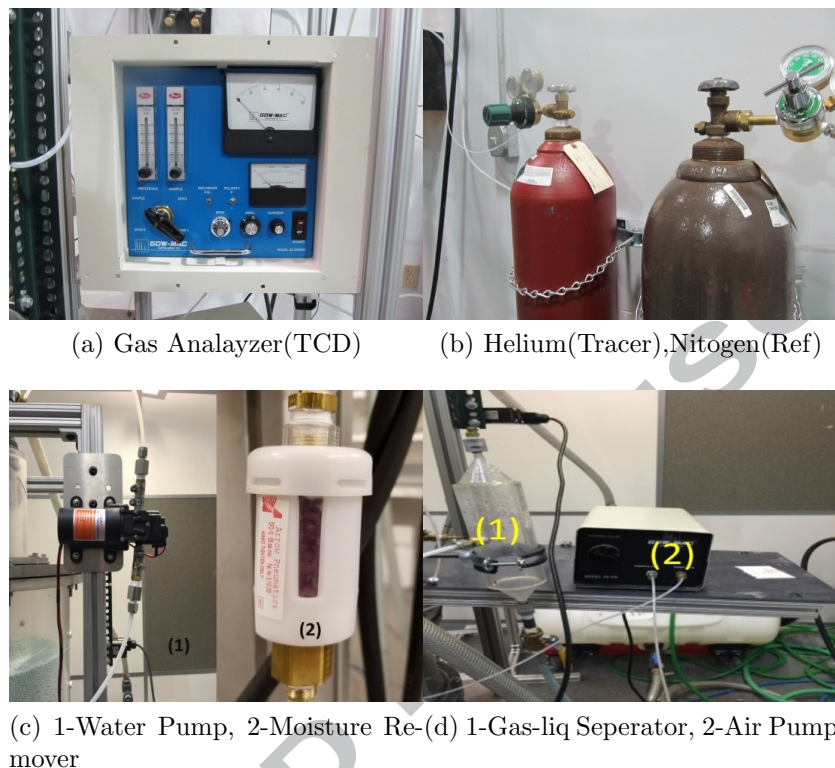


Figure 2: Gas tracer components

201 3, and after that, sampling (S) of the mixture is done using sampling tubes
 202 and water pump (Figure 2c), which draws out the mixture and feeds into
 203 an in-house developed gas-liquid separator (Figure 2c). This pump creates a
 204 suction to remove gas phase from the separator and then it passed through
 205 a moisture remover (Figure 2c), and then only gas phase to the TCD (Fig-
 206 ure 2a). The thermal conductivity of the helium mixed in the gas phase is
 207 compared with the reference gas (Nitrogen) for TCD. The helium mixture in
 208 gas has higher thermal conductivity than reference gas, and TCD response
 209 as voltage signal is linear with the concentration of helium in the air. Re-
 210 sponse from the TCD is amplified and recorded as time series at a sampling
 211 frequency of 10 Hz. Each injection will give respective RTD and will be used
 212 all together in developed methodology to determine gas dispersion parameter
 213 of the catalyst bed alone.

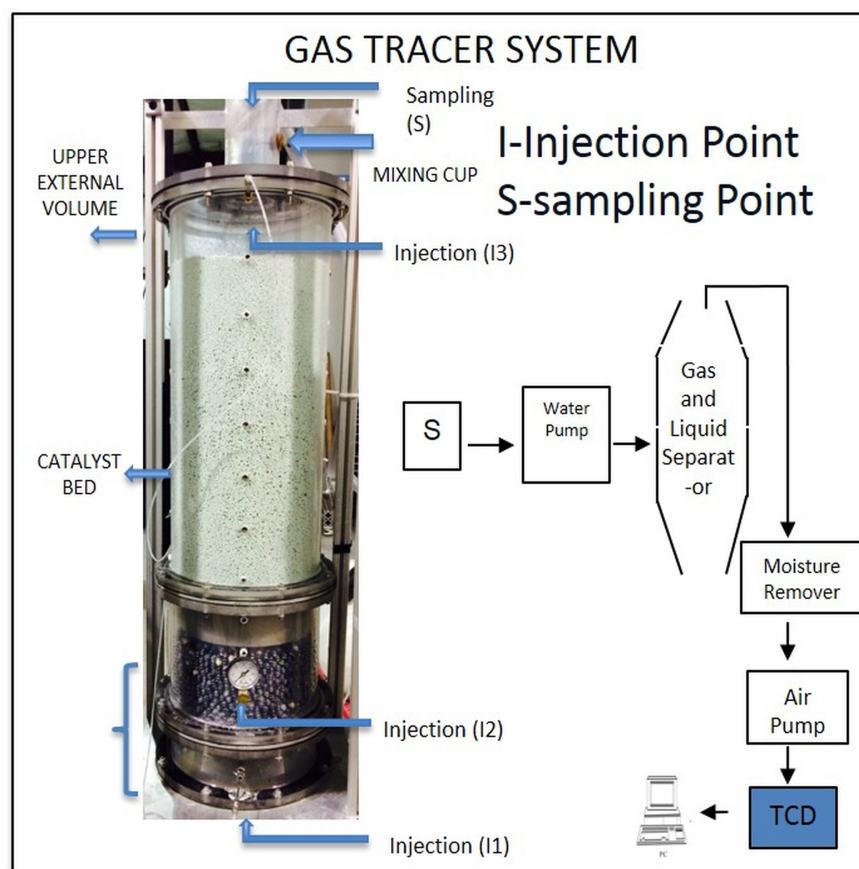


Figure 3: Gas dynamic tracer system of MBR

214 4. Methodology to Measure Gas Dispersion in Catalyst Bed Sec- 215 tion of MBR

216 A methodology is developed based on the injection-sampling concept
217 called multiple injection and one detection method, and a mathematical ap-
218 proach based on convolution and regression proposed and implemented by
219 [13]. This particular method is developed for upflow moving bed reactor
220 (MBR), but this method can be applied to any multiphase reactors with
221 plena.

Table 2: Injection and sampling assembly of MBR for gas dynamics study

| Measurement | Injection | Sampling | Dispersion Zones |
|-------------|-----------|----------|---|
| C(1) | I1 | S | Zone(1): Plena + Catalyst Bed + Upper external Volume + Sampling Line (measurement Volume) |
| C(2) | I2 | S | Zone(2): Catalyst Bed + Upper External Volume + Sampling Line (measurement volume) |
| C(3) | I3 | S | Zone(3): Upper External Volume + Sampling Line (Measurement Volume) |

222 4.1. Injection and Sampling Assembly

223 Injection-sampling assembly is designed in a way to have one point measurement (S) with three injections (I1, I2, I3) as shown in the Figure 3. Table 224 2 shows the zones covered by each injection and sampling point. The injection (I1) is at the bottom of the reactor and just below the plenum section, 225 226 injection (I2) is below the conical bottom, and injection (I3) is just above the catalyst bed as shown in the Figure 3. The sampling (S) at the top of the reactor. The measurement C(1) (I1-S) gives RTD of the entire reactor which 227 228 includes the plena, catalyst bed section, upper external volume from above the bed to sampling point, sampling assembly, and measurement system line. 229 230 The measurement C(2) (I2-S) gives the RTD of zones other than plena, and measurement C(3) (I3-S) gives the RTD of the zones other than plena and 231 232 catalyst bed section. The RTDs of each section are plotted in Figure 4 for industrial scale down conditions. 233 234 235

236 The shape of the RTD curve depends on the type of injection and flowing structure [3]. The injections are usually of the pulse, imperfect pulse, step, 237 238 sinusoidal, ramp and parabolic in nature [3]. In the majority of the studies, mixing characteristics of phases are investigated using pulse injection [3]. 239 240 In our case, we injected tracer as pulse, and if the reactor mixing behavior is between plug flow and perfectly mixed CSTR, then the response of the 241 242 system for pulse injection will be of Gauss Jordan distribution type [3], as

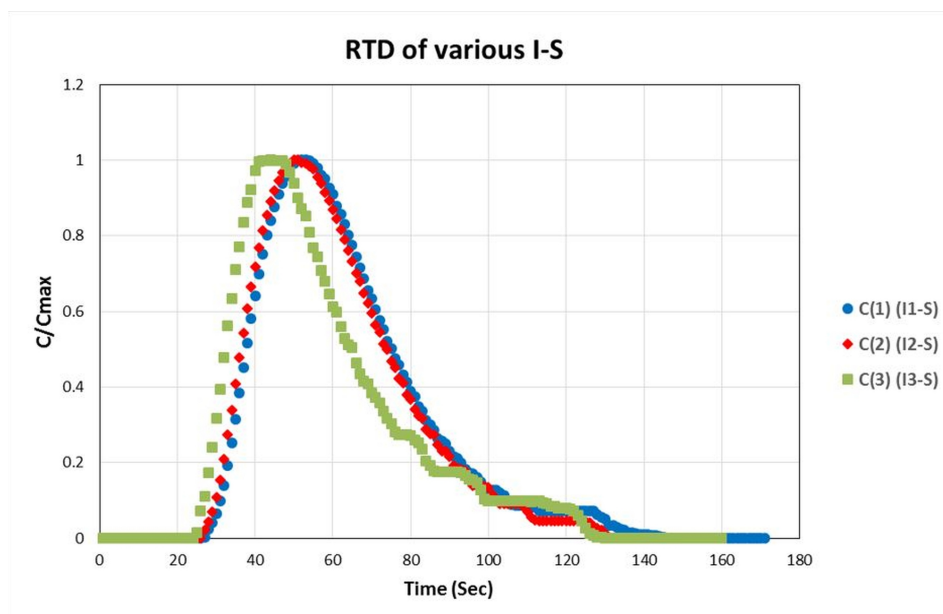


Figure 4: RTD of various injection-sampling at scaled experimental conditions

243 also observed from the Figure 4. We also observe step-like behavior towards
 244 the tail region for all the signals. This phenomenon is mainly due to the
 245 recirculation zones seen in the joint areas of upper external volume, which
 246 also consists of mixing cup (Figure 3). These recirculation's create pseudo-
 247 dead zones which leads to slow and late removal of tracer from these regions,
 248 and it can contribute towards the occurrence of step-like signals at the tail
 249 region. The tracer flows through the upper external volume to obtain all the
 250 signal C(1), C(2) and C(3), as seen from Table 2, and hence show step signal
 251 towards the tail regions. The RTD curves are usually plotted by normalizing
 252 it with its peak value [[19], [13], [14]] and are used to determine holdups,
 253 mass transfer parameters, and linear isotherms parameters [19], the same is
 254 done here. The plots are normalized based on the maximum concentration
 255 for each RTD signal.

256 4.2. Convolution and Regression Approach to Estimate Gas Dispersion in 257 Catalyst Bed of MBR

258 Convolution principle is widely used to get the RTD signal of the region
 259 which is accompanied by additional volume hence additional dispersion. De-

convolution in another mathematical way to extract out the signal of the interested zone by removing dispersion for additional volumes from the overall signal, but this method is usually not preferred in chemical engineering applications due to numerical instability [13]. Convolution integral shown by equation 1 is a mathematical way to obtain RTD of a system for any arbitrary input [3]. In equation 1, C_{in} is the inlet concentration or input and C_{out} is the response of the system and C_{out}^* is the output of this system for an inlet concentration profile of C_{in} . Both input (C_{in}) and system response (C_{out}) can be obtained by proposing a model and regression to estimate model parameters, or directly from experimental RTD for a Dirac pulse input.

$$C_{out}^* = \int_0^t C_{out}(t') \cdot C_{in}(t - t') \cdot dt' \quad (1)$$

The different regions of the reactor either additional volumes or zone of interest, can be modeled by simple or complex differential type model following diffusional type mixing or stage-wise macro-mixing model where mixing is described by perfectly staged regions [4]. The complexity of the model increases with its increase in parameter, and it tries to characterize the realistic flow pattern. Some of these models are summarized in the review of [3].

The reactor shown in Figure 3 has three regions; catalyst bed section, plena (Additional volume), upper external space plus sampling line (Additional volume). ADM is the most commonly used model for the packed bed dispersion studies, here ADM is the assumed model for the catalyst bed with two parameters D_g (Dispersion coefficient) and Gas Holdup (ϵ_g). Ideal CSTR plus PFR series is the assumed model for the plena (lower plenum, packed bed region between the conical bottom and distributor plate), as CSTR is the most commonly used model for plenum for upflow reactors ([13]), and RTD experiment gives the response of upper external volume (I3-S Figure 4). Then a single point multiple injection methods (section 4.1) is implemented along with convolution and regression to get ADM parameters. ADM is solved by two-step process, In first step; by determining the concentration for inlet boundary condition for ADM, which is the solution of ideal CSTR+PFR model (quantifies mixing in plena). In the second step; solving ADM numerically for the closed-closed boundary with inlet concentration from step 1, and parameters for regression. If the ADM or ideal CSTR plus PFR are

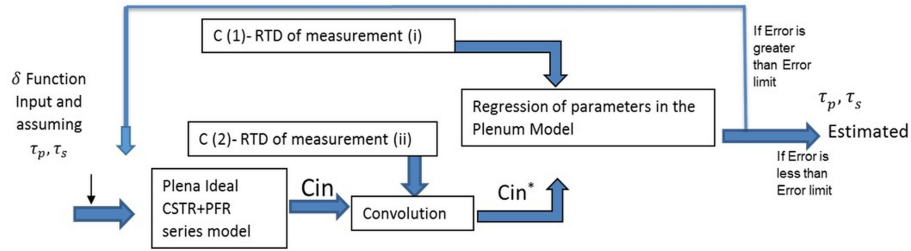


Figure 5: Schematic of convolution and regression approach to obtain parameters for plenum model

294 not a valid model to quantify the gas mixing process in catalyst bed section
 295 and plena, then it fails during regression test.

296 4.3. Step 1: Procedure to Obtain Plenum Model Parameters and Inlet Bound- 297 ary Condition for ADM

298 Figure 5 show the schematic of the procedure of step 1. The plena are
 299 taken as ideal CSTR and PFR (equation 2), and it has two parameters τ_p
 300 (Space time of PFR) and τ_s (Space time of CSTR), the parameters are at
 301 first assumed to initiate the run for step 1. The assumed parameters give
 302 C_{in} , which is theoretically input to the section zone-2 (Table 2).

$$C_{in}(t) = 0, t < \tau_p$$

$$C_{in}(t) = \left(\frac{e^{-\frac{(t - \tau_p)}{\tau_s}}}{\tau_s} \right), t > \tau_p \quad (2)$$

303 Applying convolution principle; C_{in} is the input to the Zone 2 (Table 2)
 304 and the response of the Zone-2 is measured by I2-S as shown in Figure 4,
 305 $C(2)$ is obtained experimentally by (I2-S) (Figure 4)

$$C_{in}^* = \int_0^t C_{in}(t') \cdot C(2)(t - t') \cdot dt' \quad (3)$$

306 The convolution gives C_{in}^* (Figure 6) which is the theoretical output of the
 307 zone 2 (Table 2), for an input concentration of C_{in} which represents mixing
 308 behavior of gas in plena, as shown in Figure 6. Hence C_{in}^* represents the
 309 theoretical RTD of the entire reactor (Zone 1) as it comprises of Plena and

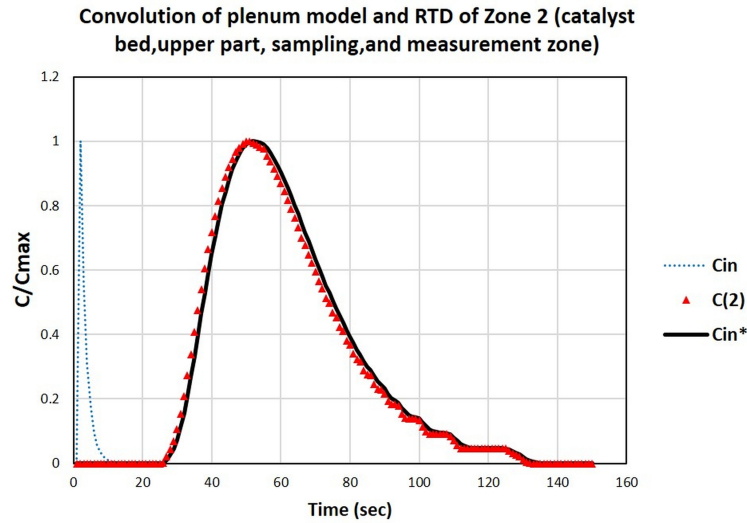


Figure 6: C_{in} (solution of plenum model; ideal CSTR+PFR), $C(2)$ (experimental response of zone-2 measured by I1-S), C_{in}^* (convoluted signal of C_{in} and $C(2)$)

310 Zone 2. Experimentally we have determined RTD for the whole reactor (Zone
 311 1) $C(1)$ by I1-S. The regression of $C(1)$ (experimental) and C_{in}^* (theoretical)
 312 for τ_p and τ_s yields these parameters for minimum error of averaged squared
 313 error in the time domain (equation 4). The n in equation 4 is the number of
 314 data points.

$$Error = \frac{1}{n} \sum_{j=1}^n [C_{in}^*(t_j) - C(1)(t_j)]^2 \quad (4)$$

315 Figure 7 shows the plot of theoretical output based on plenum model and
 316 experimental output of the whole reactor for minimum error for the equation
 317 4. The estimated regression parameter are τ_p (1sec) and τ_s (1sec) for scaled
 318 down operating conditions. The error in the equation for the estimated pa-
 319 rameter at scaled down experimental conditions is 0.00041 and this indicates
 320 that the assumed model is valid enough to represent the gas mixing in plenum.
 321 The regressed τ_p and τ_s parameter are plugged into equation 2, which is used
 322 as an initial concentration for inlet boundary condition of ADM.

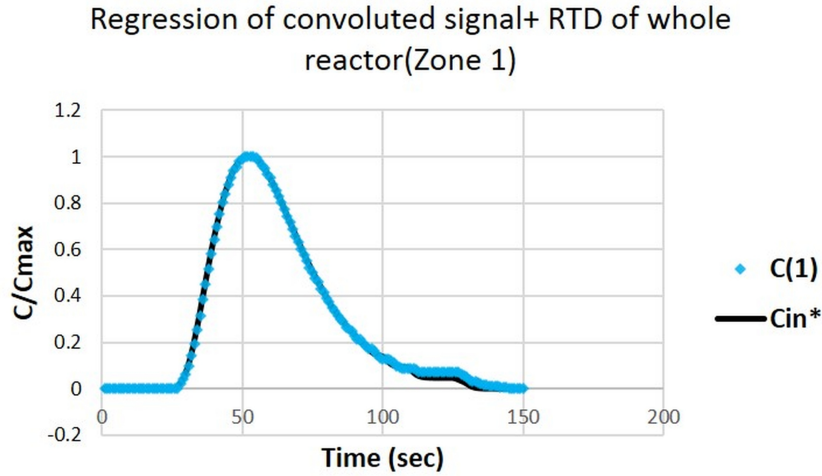


Figure 7: Regression of the theoretical output based on the plenum model (C_{in*}) and the experimental output ($C(1)$) of the whole reactor for minimum error

323 4.4. Step 2: The Procedure to Obtain ADM Model Parameters using Step 1
324 Inlet Boundary Condition

325 The catalyst bed section shown in Figure 1 and Figure 3, is modeled using
326 Axial dispersion model (equation 5) with boundary condition (equation 6 and
327 7). The parameter of ADM are D_g (gas dispersion coefficient) and ϵ_g (gas
328 holdup). The ADM is solved numerically by plugging C_{in} in equation (6)
329 from the C_{in} obtained from step 1 (Figure 5), and initiate the procedure
330 (Figure 8) by assuming the parameters (D_g , and ϵ_g). The solution of ADM
331 yields C_{out} , which is output of ADM for inlet concentration of plena as shown
332 in Figure 9. In other words C_{out} is the theoretical RTD of plena plus catalyst
333 bed section for dirac pulse input. C_{out} is also an theoretical input for Zone 3
334 (Table 2).

$$\frac{\partial C_g}{\partial t} = D_g \frac{\partial^2 C_g}{\partial Z^2} - \frac{U_g}{\epsilon_g} \frac{\partial C_g}{\partial Z} \quad (5)$$

Boundary Conditions:

$$Z = 0, U_g.C_{in} = U_g.C_g|_{z=0} - D_g \frac{\partial C_g}{\partial Z}|_{z=0} \quad (6)$$

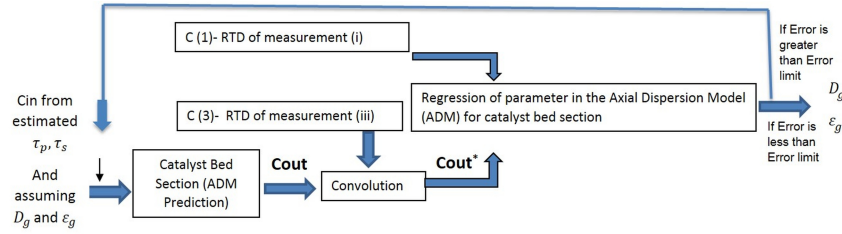


Figure 8: Schematic of convolution and regression approach to obtain parameters for ADM model using input profile C_{in}

335 Applying convolution principle (equation 8); C_{out} is the input to zone 3
 336 and C(3) is experimental response of zone 3 obtained by I3-S (Figure 4).

$$Z = L, \frac{\partial C_g}{\partial z} \Big|_{z=L} = 0 \quad (7)$$

337 The convoluted output C_{out^*} represents the output of the zone 3 for input
 338 profile C_{out} , (which represents the RTD of plenums plus catalyst bed section).
 339 Hence C_{out^*} represents the theoretical output of the entire reactor or zone 1.
 340 Experimental output of the zone-1 is obtained by C(1) (I1-S) (Figure 4).

341 The regression of C(1) (experimental) and C_{out^*} (theoretical) for D_g and ϵ_g
 342 yields these parameters for minimum error of averaged squared error in time
 343 domain (equation 9).

$$C_{out^*} = \int_0^t C_{out}(t') \cdot C_3(t - t') \cdot dt' \quad (8)$$

344 The two parameter regression by equation involves unconstrained regres-
 345 sion of parameters [19]. One of the parameter (ϵ_g) is constrained between
 346 ϵ_{gmin} and ϵ_{gmax} as shown by equation 10, this improves accuracy and speed of
 347 regression calculation. Peclet number (Pe) is also estimated using equation
 348 11.

$$Error = \frac{1}{n} \sum_{j=1}^n [C_{out^*}(t_j) - C(1)(t_j)]^2 \quad (9)$$

$$\epsilon_{gmin} = \frac{U * t_1}{L}, \epsilon_{gmax} = \frac{U * t_2}{L} \quad (10)$$

349 Whereas, U is superficial velocity of gas based on empty column, L is the

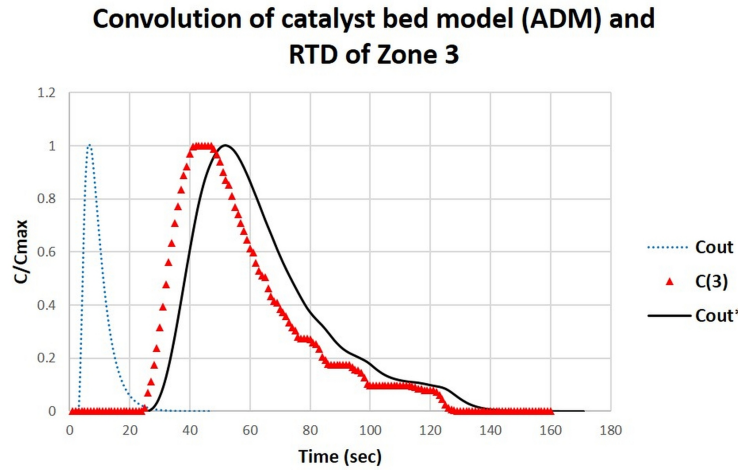


Figure 9: C_{out} (ADM solution of plenum model input), $C(3)$ (experimental output of zone1), C_{out*} (convoluted signal output of C_{out} and RTD of zone3)

350 linear distance between injection (I2 and I3), t_1 is time difference between
 351 first signal arriving for C(2) and C(3), and t_2 is the time difference between
 352 mean residence time (equation 16) for C(2) and C(3), ϵ_g is the gas holdup in
 353 packed bed, D_g is the gas dispersion coefficient.

$$Pe = \frac{U * L}{\epsilon_g * D_g} \quad (11)$$

354 Figure 10 shows the regression for minimum error of equation 9 for pa-
 355 rameter D_g and ϵ_g . The estimated regression parameters are D_g ($0.1m^2/s$), ϵ_g
 356 (0.0823), and Pe (7.87) for scaled down operating conditions. The minimum
 357 error for experimental scaled down condition is 0.00051 , which is lower than
 358 the tolerance limit of 0.001 , and hence validates that the ADM is a valid
 359 model to represent gas dynamics in catalyst bed of MBR. This methodology
 360 is applicable for the catalyst bed section of the MBR reactor for gas dynamics
 361 investigation. In addition to these parameters, dimensionless variance (σ_D^2)
 362 is calculated for the bed section of MBR using the RTDs (Table 2), which
 363 also indicates the degree of mixing, with σ_D^2 of zero indicates plug flow and
 364 σ_D^2 of one indicates complete mixing.

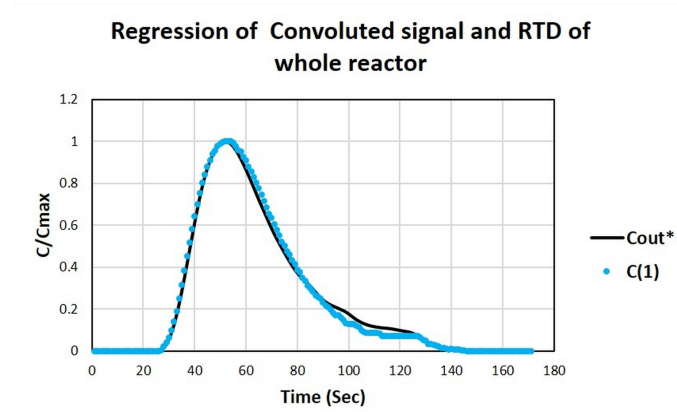


Figure 10: Regression plot of C_{out^*} (convoluted signal of ADM output and experimental output of zone-3 (I3-S)) and $C(1)$ (experimental output of zone1) for minimum error

365 5. Dimensionless Variance (Tank in Series)

366 Tank in series is modeling concept, where n tanks are modeled as ideal
 367 CSTR in series for pulse injection of tracer. The theoretical residence time
 368 distribution (RTD) obtained from the model is regressed with experimental
 369 RTD of non-ideal reactor by varying the number of tank (n). Larger the
 370 value of n indicating the flow is towards plug flow and lower means the flow
 371 is towards CSTR. [20] showed that equation 12 is the generalized RTD for n
 372 tank modeled as ideal CSTR in series.

$$E(t) = \frac{t^n}{(n-1)!\tau_i^n} e^{-t/\tau_i} \quad (12)$$

373 Where τ_i is the means residence time in single tank, n is the number of
 374 tank, and τ_i is equal to τ/n , and τ is mean residence time of entire reactor.
 375 Equation 12 is converted to dimensionless form $E(\theta)$ as shown in Equation
 376 13.

$$E(\theta) = \tau E(\theta) = \frac{n(n\theta)^{n-1}}{(n-1)!} e^{-n\theta} \quad (13)$$

377 Where θ is the ratio of t and τ . The variance of equation 13 can be
 378 found using equation 14, which is called dimensionless variance (σ_D^2), and
 379 this dimensionless variance is equal to the ratio of variance (σ^2) and square

380 of mean residence time (t_m).

$$\sigma_D^2 = \frac{\sigma^2}{t_m^2} = \int_0^\infty (\theta - 1)^2 E(\theta) d\theta \quad (14)$$

381 [20] showed the solution of equation 14 is equal to the inverse of number
382 of tanks (n), as shown in equation 15.

$$\sigma_D^2 = \frac{\sigma^2}{t_m^2} = \frac{1}{n} \quad (15)$$

383 This indicates if σ_D^2 is zero then n is infinity, which is the case for plug
384 flow, and when σ_D^2 is one then n is one, which means complete mixing.
385 Dimensionless variance can be determined by RTD experiments, as it is the
386 ratio of variance (σ^2) (second moment) and square of mean residence time
387 (t_m) (first moment).

$$\text{MeanResidenceTime}(t_m) = \int_0^\infty E(t) t dt \quad (16)$$

$$\text{Variance}(\sigma^2) = \int_0^\infty (t - t_m)^2 E(t) dt \quad (17)$$

388 In our case, the area of interest is packed bed region, and its dimensionless
389 variance is evaluated by finding the variance of RTD of zone 2 (t_{m2}) (Figure
390 4 and Table 2) and RTD of zone 3 (t_{m3}) (Figure 4 and Table 2) using the
391 equation 16 and similarly the variance (σ_2^2 and σ_3^2) using equation 17. Volume
392 of Zone 2 minus volume of zone 3 gives volume of bed, and as these moments
393 are additive the bed variance will be ($\sigma_2^2 - \sigma_3^2$) and mean residence time in
394 the bed will be ($t_{m2} - t_{m3}$). Hence the σ_D for the bed is calculated using
395 equation 18.

$$\sigma_D^2(\text{Bed}) = \frac{(\sigma_2^2 - \sigma_3^2)}{(t_{m2} - t_{m3})^2} \quad (18)$$

396 Equation 18 shows the dimensionless variance of the gas phase in catalyst
397 bed region and for scaled down experimental condition (Table 1), σ_D^2 is 0.232.

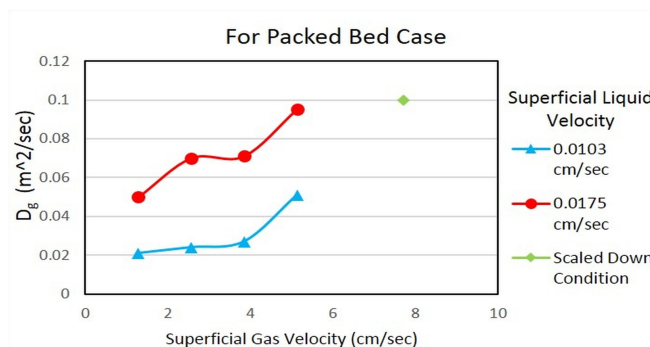
398 6. Results and Discussion

399 Gas transport inside a reactor with packing is mainly occurring due to
400 three mechanism; bulk flow due to pressure gradients, diffusion due to concen-

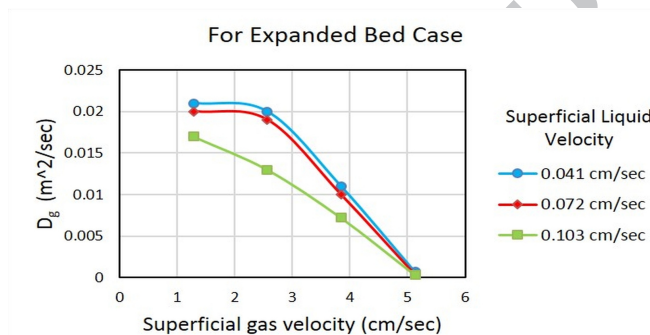
401 tration gradients, and convective dispersion due to spatial velocity fluctuation
 402 [21]. The summation of last two parameters defines the dispersion/mixing
 403 of phase in the system. The D_g values estimated from ADM equation is a
 404 lumped parameter indicating both molecular diffusion and convective dis-
 405 persion (hydrodynamic mixing) [12] in 3-dimensional space of catalyst bed.
 406 Hence, our focus of this study is to see dispersion/mixing behavior of gas in
 407 terms of D_g values. The value of D_g functionally depends on the ratio of the
 408 particle diameter to column diameter, fluid density and viscosity, superficial
 409 velocities of phases, ratio of the length of the reactor to the column diame-
 410 ter, particle size distribution, and effect of temperature [8]. In this study, we
 411 wanted to see the effect of superficial velocity on the dispersion coefficient
 412 (D_g), pecelet number (Pe), and dimensionless variance (σ_D^2) in the catalyst
 413 bed section of MBR.

414 6.1. Effect of Flow Rate of Phases on Gas Dispersion Coefficient (D_g) for 415 Catalyst Bed in MBR

416 Figure 11 shows the trend in D_g values for varying superficial velocity
 417 of the gas at low liquid superficial velocities (Figure 11a) and at high liq-
 418 uid superficial velocities (Figure 11b). Figure 11a shows that the D_g values
 419 are increasing with increase in gas flow rate and liquid flow rates, and this
 420 phenomenon is usually observed in packed bed reactor [[12], [8], [14]]. To
 421 understand the effect of velocity on D_g in packed bed, let us look into the
 422 equation $D_l = D_m' + ud/Pe_L(\infty)$ [[22], [12], [8]]. For packed bed, the es-
 423 timated D_g is the summation of molecular diffusivity (D_m') and dispersion
 424 due to turbulent or eddy motion of flow i.e, convection ($ud/Pe_L(\infty)$). At
 425 low particle Reynolds number; less than 1.8 for gases, molecular diffusivity
 426 plays a vital role (Edward 1968). On increasing the velocity, the flow moves
 427 towards the turbulent flow, and eddy diffusion plays a dominant role in gas
 428 transport due to spatial velocity variations and fluctuations. The dispersive
 429 component due to eddy diffusion ($ud/Pe_L(\infty)$), depends on interstitial ve-
 430 locity which in turn depends on packing structure, flow distribution, and flow
 431 rates. Hence, increase in flow rate increases the convective dispersion com-
 432 ponent ($ud/Pe_L(\infty)$), and also results in the increase in bubble breakage
 433 phenomena due to the interaction of gas bubbles with catalyst bed particles
 434 ([23]). Hence, on increasing gas flow rate, we observe wider bubble size dis-
 435 tribution which results in wider spread of gas phase along the 3-dimensional
 436 space of catalyst bed and increased mixing due to the convective component
 437 of dispersion. Both of these mechanism leads to increase in the estimated D_g



(a) Plots of D_g for varying flow rate of gas at low liquid velocity



(b) Plots of D_g for varying flow rate of gas at high liquid velocity

Figure 11: Gas dispersion plot for varying flow rate of phases

438 value with increase in gas flow rate. From dispersion/mixing point of view
 439 increasing the gas velocity at low liquid flow rate is good, as it increases the
 440 overall mixing, reduces channeling [12], provides better radial distribution
 441 [14]. At scaled down experimental condition, visually, the bed is behaving
 442 in packed bed state with slight expansion at the top of the bed. The results
 443 (Figure 11a) also confirm that the bed is behaving as packed for these flow
 444 rates. The gas phase flow dynamics completely change when the bed starts
 445 to expand and which we observed for the higher flow rate of the liquid.

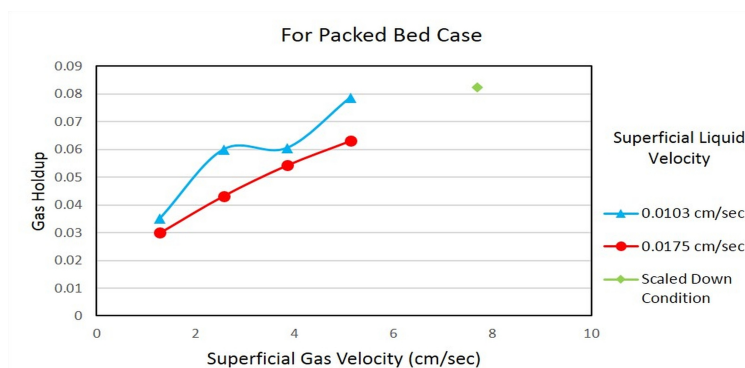
446 Figure 11b shows decreasing trend of D_g value with increase in both gas
 447 and liquid flow rates, which is complete opposite trend of the phenomena
 448 observed for packed bed case (Figure 11a). It shows the bed is not anymore

449 in packed bed state and the bed expansion is significant at the higher flow
450 rate of liquid [19] which promotes backmixing. It is seen that with the
451 increase in gas and liquid velocities result in more expansion of the bed and
452 bed flow dynamics move towards the 3-phase fluidized bed. At expanded
453 bed conditions the gas phase can displace suspended solid phase and gas
454 phase follows least resistance path, which results in a less cross-sectional
455 distribution of gas phase at these conditions. Although overall the bed is
456 at high turbulent condition due to movement of solid particles, but due to
457 less spread of gas phase along the cross-section results in the reduction in
458 estimated values of D_g . In terms of mixing this condition is not good for
459 hydrotreating applications. As the bubbles try to coalesce and move without
460 dispersing cross-sectionally, which results in inefficient utilization of catalyst.
461 Hence it is desired to run this reactor at the conditions of packed bed with
462 least and preferably no expansion of the bed. By looking at the trend of D_g
463 value for expanded bed, it looks the flow is more towards the plug flow state.
464 Usually in three-phase fluidized bed the gas phase flow as plug flow with
465 significant backmixing of the liquid phase [24]. To see how much deviation the
466 gas flow is from plug flow, Pe and σ_D^2 evaluation is needed. To estimate Pe ,
467 ϵ_g values are needed. For three phase flow, ϵ_g is the function of flow rate and
468 packing [25] and is one of the estimated parameter from the ADM equation
469 5 which is discussed in section 4.4, and its variation with flow conditions are
470 measured to calculate Pe (Equation 11).

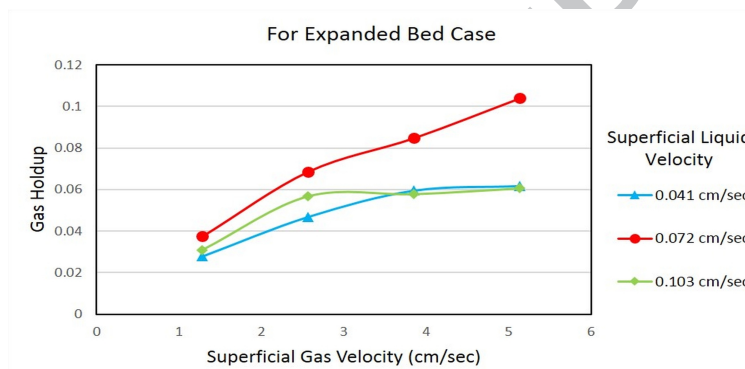
471 6.2. Effect of Flow Rate of Phases on the Gas Holdup (ϵ_g) in Catalyst Bed 472 of MBR

473 From dispersion plot (Figure 11), we were able to identify the flow rates
474 at which the bed behaves as packed and expanded bed, respectively. The gas
475 holdup results are also shown for packed bed (Figure 12a) and for expanded
476 bed (Figure 12b). Figure 12a shows that with the increase in gas flow rate
477 there is an increase in the gas holdup and with the increase in liquid flow rate
478 there is a decrease in the gas holdup. This behavior is expected in packed bed
479 reactor [26], as increasing gas flow rate results in better radial distribution
480 of gas phase [14] and thus increasing the residence time of the gas phase,
481 and increased residence time is equivalent to increase in the gas holdup for
482 flowing system. When the liquid flow rate is increased, the gas phase moved
483 out quickly and reduces the residence time hence reduces the gas holdup [26].

484 Figure 12b shows the gas holdup at expanded bed state for varying flow
485 rate of phases. The trend of the gas holdup is increasing with gas flow



(a) The gas holdup plot for varying gas flow rate at low liquid flow rates



(b) The gas holdup plot for varying gas flow rate at high liquid flow rate

Figure 12: Gas holdup plot for varying flow rate of phases

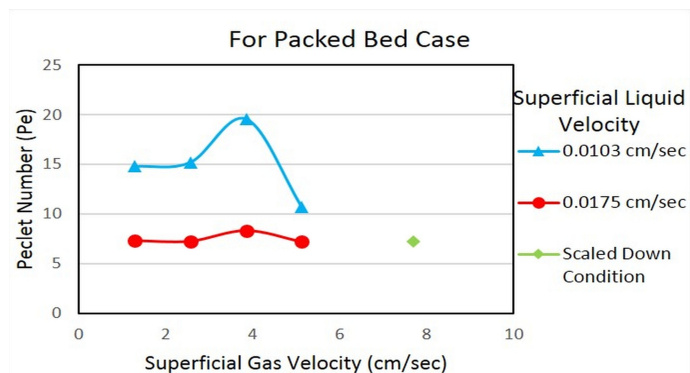
486 rate, similar to packed bed case. With the increase in liquid velocity, the
 487 trend is fluctuating. On increasing the liquid velocity from 0.0041 cm/sec to
 488 0.072 cm/sec the gas holdup increases, and from increasing the liquid velocity
 489 from 0.072 cm/sec to 0.103 cm/sec the gas holdup decreases, this kind of
 490 trend is due to the degree of bed expansion. When the flow is increased
 491 from 0.0041 cm/sec to 0.072 cm/sec , the bed expands and reduces the solid
 492 concentration [27], which in turns increases the gas holdup, as much more
 493 voidage is available for gas to distribute. As the bed is in the expanded
 494 state, hence, we expected the gas holdup to increase further when the liquid
 495 velocity is increased from 0.072 cm/sec to 0.103 cm/sec , but the gas holdup

496 decreased, and it is due to bed behavior shifts more towards the three-phase
497 fluidized bed. At this state the bed is expanded, thus the solids are easily
498 displaced by moving gas phase, and on increasing the gas velocity results
499 in bubble coalescence and movement through least resistance path, which
500 results in increased bubble rise velocity and further reduction in gas holdup
501 [[27], [28]].

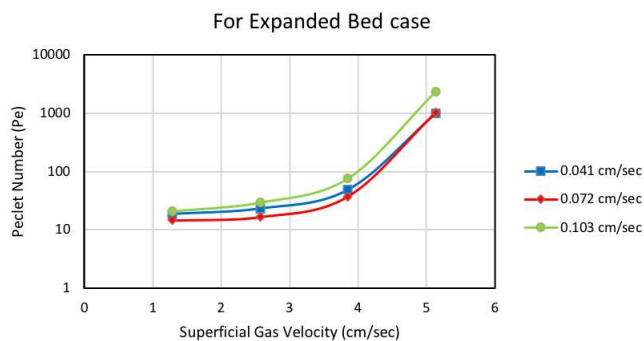
502 For hydrotreating purpose, gas to liquid mass transfer on the catalyst
503 surface is the rate-limiting step, and for high utilization of catalyst, high gas
504 holdup at high solid concentration is required, which is observed at scaled
505 down conditions. Based on the results this is occurring at low liquid and
506 high gas flow rate where the bed is behaving as packed bed.

507 6.3. Effect of Flow Rate of Phases on Peclet Number (Pe) in Catalyst Bed 508 of MBR

509 Using the D_g and ϵ_g values, Pe is calculated using equation 11. Pe is
510 a dimensionless number which gives the information of the dominance of
511 transport mechanism between bulk flow and dispersive force. Higher the Pe
512 means bulk flow forces dominate the transport, and lower Pe indicate the
513 dispersion dominates flow through the bed. Figure 13a shows the trend of
514 Pe variation for varying flow rate of gas and liquid phase, and at these flow
515 rates, the bed behaves as a packed bed. Figure 13b shows the trend of Pe
516 variation with the varying flow rate of gas and liquid phase at which the bed
517 is in the expanded state. Figure 13a trends show that the Pe is not varying
518 much with the increase in gas flow rate and decreases with increase in liquid
519 flow rate. With the increase in gas phase the dispersive forces are increases as
520 observed in Figure 11a, but this increase is due to the convective dispersion
521 component of (D_g). It indicates that at these flow rates the increase in
522 disperse force is proportional to the increase in bulk flow force and making
523 the Pe values almost constant. With the increase in liquid flow rate, the
524 gas dispersion is increased, as observed in Figure 11a and Pe number is also
525 increase (Figure 13). It means at similar gas flow rate for higher liquid flow
526 rate dispersive forces are dominating for gas transport for packed bed case,
527 which increases overall gas dispersion/mixing in the bed. Figure 13b trend
528 shows that with increasing gas flow rate for any liquid flow rate, the Pe
529 increases, which means bulk forces are dominating the transport mechanism.
530 With increases in liquid flow rate, the Pe varies but is again depended on
531 the degree of expansion. Overall as the bed moves towards 3 phase fluidized
532 bed the Pe increases which means reduced dispersion/mixing of gas phase or



(a) Peclet Number plot for varying flow rate of gas at low liquid flow rate



(b) Peclet Number plot for varying flow rate of gas at high liquid flow rate

Figure 13: Peclet number plot for varying flow rate of phases

533 moving towards plug flow. The results indicate that gas dispersion/mixing is
 534 better at packed state for higher liquid flow rate and at the higher gas flow
 535 rate. The scaled down conditions (Figure 13a) in terms of mixing is good,
 536 as it comes under the purview of packed bed with slight expansion at the
 537 top. At these flow rate, the gas mixing is good, but overall gas distribution
 538 is largely function of plena and bed packing. To confirm the findings from
 539 the results of D_g and Pe . A dimensionless variance (σ_D^2) is calculated for the
 540 bed section, which also indicates the dispersion/mixing behavior of phases.

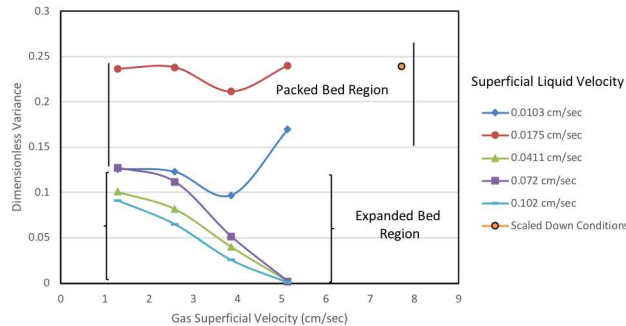


Figure 14: Dimensionless variance of gas phase in the catalyst bed for various flow conditions and scaled down conditions

541 *6.4. Effect of Flow Rate of Phases on Dimensionless Number (σ_D^2) in Cat-*
 542 *alyst Bed of MBR*

543 The dimensionless variance for the catalyst bed section is calculated from
 544 the RTDs using its moments (t_m , σ^2), as explained in the section 4.1. If its
 545 values is zero then it means the gas movement is in plug flow manner, and if
 546 its one then the flow is completely mixed. Figure 14 shows the dimensionless
 547 variance in the catalyst bed for various flow condition and at scaled down
 548 conditions and it also indicates packed/expanded bed operating condition.
 549 Overall for all the flow condition the values are close to zero, indicating the
 550 gas flow is closer to plug flow. As for σ_D^2 less than 0.1 is usually considered to
 551 be in plug flow of packed bed reactor [29]. Relatively, gas dispersion/mixing
 552 is more in packed bed region, and in this region increasing liquid velocity and
 553 gas velocity increases dispersion/mixing, and in the expanded bed region the
 554 flow is moving closer to plug with increase of both gas and liquid velocities.
 555 The results are similar to what we observed from the results of Dispersion
 556 (Figure 11) and Peclet number (Figure 13). The gas dispersion/mixing is
 557 higher in the packed bed region and even for scaled down condition compared
 558 to the expanded bed regions.

559 **7. Remarks**

560 Gas dispersion/mixing has been investigated for the catalyst bed sec-
 561 tion of the pilot-scale upflow moving bed hydrotreater reactor (MBR), using
 562 injection-sampling concept based on multiple injection and detection method,

563 and a mathematical approach of convolution and regression, with appropri-
564 ate model for catalyst bed and plena proposed by [13]. The catalyst bed is
565 Modeled with Axial Dispersion Model (ADM), with its inlet boundary condi-
566 tion obtained from the Ideal CSTR plus PFR model of plena, these models
567 are assumed first and validated based on the regression. This methodology
568 is successfully implemented in the MBR at the scaled-down experimental
569 condition and various other flow rates of phases. The dispersion plot indi-
570 cates that at low liquid flow rates the D_g increases with increases in gas flow
571 rate and decreases with increase in liquid flow rate, this trend is observed in
572 packed bed state. At higher liquid flow rates the D_g is decreasing with in-
573 crease in both gas and liquid flow rate, and this trend is observed in expanded
574 bed state. Pe plot shows that the in packed bed state the flow is relatively
575 dominated by the dispersive forces and in expanded bed state gas flow moves
576 towards plug flow state with the increase in bed expansion. This is confirmed
577 by calculating σ_D^2 , which indicate overall the gas phase flow is towards plug
578 flow, but at expanded bed state the flow is more closer to plug flow. Hence,
579 a good gas mixing is achieved for highest flow condition of phases where the
580 bed expansion is minimum, and that is seen in the scaled-down experimental
581 condition.

582 8. Acknowledgments

583 The authors like to acknowledge the financial and technical support given
584 by Kuwait Institute for Scientific Research (KISR), Kuwait National Petroleum
585 Company (KNPC) and Kuwait Petroleum Corporation (KPC). Authors also
586 like to acknowledge Dr. Lu Han and Dr. Rahman Abdulmohsin, for their
587 efforts in developing the methods and experimental setup related to gaseous
588 tracer technique available at Department of Chemical Engineering, Missouri
589 S&T.

- 590 [1] A. Toukan, V. Alexander, H. Albazzaz, M. Al-Dahhan, Identification
591 of flow regime in a cocurrent gas-liquid upflow moving packed bed reac-
592 tor using gamma ray densitometry, *Chemical Engineering Science* 168
593 (2017) 380–390.
- 594 [2] E. R. Bruce, E. S. Bruce, K. Parimi, Gas pocket distributor for hydropro-
595 cessing a hydrocarbon feed stream, US Patent, US5885534A (1999).

- 596 [3] Y. T. Shah, G. J. Stiegel, M. M. Sharma, Backmixing in gas-liquid
597 reactors, *AIChE Journal* 24 (1978) 369–400.
- 598 [4] I. Iliuta, F. C. Thyron, O. Muntean, Axial dispersion of liquid in gas-
599 liquid cocurrent downflow and upflow fixed-bed reactors with porous
600 particles, *Chemical Engineering Research and Design* 76 (1998) 64–72.
- 601 [5] J. H. Koh, P. C. Wankat, N. H. L. Wang, Pore and surface diffusion
602 and bulk-phase mass transfer in packed and fluidized beds, *Industrial
603 and Engineering Chemistry Research* 37 (1998) 228–239.
- 604 [6] L. Valenz, F. J. Rejl, V. Linek, Gas and liquid axial mixing in the
605 column packed with Mellapak 250Y, Pall rings 25, and intalox saddles
606 25 under flow conditions prevailing in distillation columns, *Industrial
607 and Engineering Chemistry Research* 49 (2010) 10016–10025.
- 608 [7] A. H. Benneker, A. E. Kronberg, J. W. Post, A. G. J. Van Der Ham,
609 K. R. Westerterp, Axial dispersion in gases flowing through a packed
610 bed at elevated pressures, *Chemical Engineering Science* 51 (1996) 2099–
611 2108.
- 612 [8] J. M. P. Q. Delgado, A critical review of dispersion in packed beds, *Heat
613 and Mass Transfer/Waerme- und Stoffuebertragung* 42 (2006) 279–310.
- 614 [9] K. Muroyama, L.-S. Fan, Fundamentals of gas-liquid-solid fluidization,
615 *AIChE Journal* 31 (1985) 1–34.
- 616 [10] A. K. Saroha, R. Khera, Hydrodynamic study of fixed beds with cocur-
617 rent upflow and downflow, *Chemical Engineering and Processing: Pro-
618 cess Intensification* 45 (2006) 455–460.
- 619 [11] O. Levenspiel, W. Smith, Notes on the diffusion-type model for the
620 longitudinal mixing of fluids in flow, *Chemical Engineering Science* 6
621 (1957) 227 – 235.
- 622 [12] M. Edwards, J. Richardson, Gas dispersion in packed beds, *Chemical
623 Engineering Science* 23 (1968) 109 – 123.
- 624 [13] L. Han, Hydrodynamics and mass transfer in slurry bubble column, PhD
625 Thesis, 2007.

- 626 [14] R. S. Abdulmohsin, M. H. Al-Dahhan, Axial dispersion and mixing
627 phenomena of the gas phase in a packed pebble-bed reactor, *Annals of*
628 *Nuclear Energy* 88 (2016) 100–111.
- 629 [15] A. Carleton, R. Flain, J. Rennie, F. Valentin, Some properties of a
630 packed bubble column, *Chemical Engineering Science* 22 (1967) 1839 –
631 1845.
- 632 [16] N. Midoux, J. C. Charpentier, On an experimental method of residence
633 time distribution measurement in the fast flowing phase of a two-phase
634 flow apparatus: Application to gas flow in gas-liquid packed column,
635 *The Chemical Engineering Journal* 4 (1972) 287–290.
- 636 [17] P. Danckwerts, Continuous flow systems: Distribution of residence
637 times, *Chemical Engineering Science* 2 (1953) 1 – 13.
- 638 [18] M. Simcik, M. C. Ruzicka, A. Mota, J. A. Teixeira, Smart rtd for
639 multiphase flow systems, *Chemical Engineering Research and Design* 90
640 (2012) 1739–1749.
- 641 [19] J. Yun, S. J. Yao, D. Q. Lin, Variation of the local effective axial disper-
642 sion coefficient with bed height in expanded beds, *Chemical Engineering*
643 *Journal* 109 (2005) 123–131.
- 644 [20] H. S. Fogler, *Elements of chemical reaction engineering* 4th Edition
645 (2005).
- 646 [21] L. Pugliese, T. G. Poulsen, R. R. Andreasen, Relating Gas Dispersion
647 in Porous Media to Medium Tortuosity and Anisotropy Ratio, *Water,*
648 *Air, & Soil Pollution* 223 (2012) 4101–4118.
- 649 [22] D. J. Gunn, C. Pryce, Dispersion in Packed Beds, *Trans Inst Chem*
650 *Eng* 47 (1969) t341–t350.
- 651 [23] L. A. Briens, N. Ellis, Hydrodynamics of three-phase fluidized bed sys-
652 tems examined by statistical, fractal, chaos and wavelet analysis meth-
653 ods, *Chemical Engineering Science* 60 (2005) 6094–6106.
- 654 [24] L. S. Fan, F. Bavarian, R. L. Gorowara, B. E. Kreischer, R. D. Buttke,
655 L. B. Peck, Hydrodynamics of gas-liquid-solid fluidization under high
656 gas hold-up conditions, *Powder Technology* 53 (1987) 285–293.

- 657 [25] A. Beg, M. Hassan, M. Naqvi, Hydrodynamics and mass transfer in
658 a cocurrent packed column a theoretical study, *Chemical Engineering*
659 *Journal and the Biochemical Engineering Journal* 63 (93-103) 1–2.
- 660 [26] J. H. P. Collins, A. J. Sederman, L. F. Gladden, M. Afeworki, J. Dou-
661 glas Kushnerick, H. Thomann, Characterising gas behaviour during
662 gas-liquid co-current up-flow in packed beds using magnetic resonance
663 imaging, *Chemical Engineering Science* 157 (2017) 2–14.
- 664 [27] S. Kumar, R. A. Kumar, P. Munshi, A. Khanna, Gas hold-up in three
665 phase co-current bubble columns, *Procedia Engineering* 42 (2012) 782–
666 794.
- 667 [28] H. M. Jena, G. K. Roy, B. C. Meikap, Prediction of gas holdup in a three-
668 phase fluidized bed from bed pressure drop measurement, *Chemical*
669 *Engineering Research and Design* 86 (2008) 1301–1308.
- 670 [29] D. Tang, J. A., R. X., B. B., S. S., Axial dispersion and wall effects in
671 narrow fixed bed reactors: A comparative study based on rtd and nmr
672 measurements, *Chemical Engineering & Technology* 27 (2004) 866–873.

Highlights

- Estimation of Gas Mixing/Dispersion Parameter (D_g, Pe, σ_D^2) for catalyst bed
- At low liquid flow rate, the bed is in packed bed and it expands for increasing flow
- Gas mixing/dispersion is higher in packed bed state
- For all flow conditions, the gas flow is not deviating much from plug flow
- Scaled down flow condition is good in terms of mixing and catalyst utilization